# Remarkable spreading behavior of molybdena on silica catalysts. An *in situ* EXAFS-Raman study

M. de Boer *, A.J. van Dillen, D.C. Koningsberger, J.W. Geus

*Department of Inorganic Chemistry, University of Utrecht, Sorbonnelaan 16, 3508 TB Utrecht, the Netherlands*

M.A. Vuurman and I.E. Wachs

*Zettlemoyer Center for Surface Studies and Department of Chemical Engineering, Lehigh University Bethlehem PA, U.S.A.*

Received 14 August 1991; accepted 26 September 1991

In contrast to the frequently reported lack of interaction between hexavalent molybdenum and $SiO_2$ and the tendency of silica-supported $MoO_3$ to coalescence, it has been found that on dehydration small molybdenum oxide clusters spread over a silica support. A combined Raman spectroscopy-X-ray absorption study shows a significantly altered structure of the molybdenum oxide phase after dehydration. In EXAFS the total Mo-Mo coordination number drops from 3.27 to 0.20 after an *in situ* thermal treatment at 673 K. The increase of the peak in the XANES region (1s → 4d) indicates that the coordination sphere of the molybdenum atoms strongly alters after dehydration. The Raman spectra reflect the change of the structure through a shift of the position of the terminal Mo=O bond from 944 to 986 $cm^{-1}$ and the disappearance of the bridged Mo-O-Mo vibration at 880 $cm^{-1}$. It is concluded that dehydration produces almost isolated molybdenum sites in this highly dispersed sample. Water ligands stabilize the oligomeric clusters under ambient conditions; the removal of water causes spreading of these clusters.

**Keywords:** Spreading; dehydration; molybdenum oxide; silica; EXAFS; Raman spectroscopy; preparation; clusters

## 1. Introduction

The preparation of supported molybdena catalysts has received much interest in the literature. The broad industrial applications of molybdena containing catalysts have resulted in many publications dedicated to the preparation and the spreading behavior of molybdena in these catalysts [1–8]. A recent study of Leyrer et al. [9] on $MoO_3$ on $Al_2O_3$ and on $SiO_2$ showed that spreading occurs on alumina surfaces over macroscopic distances (i.e., several hundreds of

micrometers), but spreading did not take place on a silica support. This observation (usually referred to as 'solid-solid wetting') agrees with many studies on the solid-solid interaction between $MoO_3$ and $Al_2O_3$ or $SiO_2$. The role of water vapor appears to be essential. Water vapor promotes the solid-solid wetting of $MoO_3$ and $Al_2O_3$ [9]. However, more recent *in situ* Raman studies with $MoO_3/TiO_2$ revealed that solid-solid wetting also occurs in the absence of moisture, but is accelerated by its presence [10].

The solid-solid interaction determines the structures of fresh silica- and alumina-supported $MoO_3$ catalysts. Generally, it has been found that alumina-supported $MoO_3$ catalysts of a high dispersion can be obtained up to high loadings [2,8,11], but that the formation of $MoO_3$-crystallites occurs at significantly lower loadings in $SiO_2$-supported catalysts. The difference in interaction between the metal precursor (usually $Mo_7O_{24}^{6-}$ from ammonium heptamolybdate (AHM)), dissolved in water, and the alumina and silica supports brings about the difference in dispersion. *To a rough first approximation it can be stated that the interaction between the precursor and the support depends on the sign of the surface charge of the support and of the dissolved complexes of the precursor.* Accordingly, $SiO_2$ (isoelectrical point (i.e.p.) $\sim 2$) behaves like an acid support as compared to $Al_2O_3$ (i.e.p. $\sim 7$). At the pH of an AHM solution ($\sim 5.5$), the interaction between the anionic heptamolybdate clusters and the positively charged $Al_2O_3$-surface is better than between the clusters and the $SiO_2$-surface, which is negatively charged. This leads to spreading of the molybdena phase over $Al_2O_3$. Many authors have speculated about the nature of the interaction between $MoO_3$ and oxidic supports, the reaction of heptamolybdate with surface hydroxyls, and the reaction (spreading) to even monomeric surface species [12–14]. Abundant evidence has been published for the high dispersion of these alumina-supported molybdena catalysts using FTIR [15], Raman spectroscopy [7,12], UV [12,16] and EXAFS [14].

Because of the lack of interaction between heptamolybdate and $SiO_2$, formation of $MoO_3$-crystallites in $MoO_3/SiO_2$ catalysts occurs at low loadings, as frequently reported [1,2,7,11,17]. Due to the poor interaction between heptamolybdate and $SiO_2$ during the preparation, large agglomerates of molybdenum oxide easily develop. During drying and calcination, these crystallites tend to further coalescence due to the high solubility of the hexavalent molybdenum species in water (ripening), and the volatility of $MoO_2(OH)_2$. As a consequence, the dispersion of silica-supported catalysts is not very stable and usually these catalysts exhibit bulk $MoO_3$ features in catalytic test reactions.

A number of authors have disclosed the influence of water on the dispersion of supported molybdenum oxide [2,7–9,11]. It is generally accepted that water promotes the dispersion of molybdena on the surface of $Al_2O_3$. Various mechanisms for this process have been proposed. Gas-phase transport through the volatile $MoO_2(OH)_2$ can be excluded at temperatures below 773 K [8]. The dispersion of a $MoO_3$ on $Al_2O_3$ catalyst increases upon treatment with water

vapor. In $MoO_3$ on $SiO_2$ catalysts, on the contrary, the effect of moisture is assumed to deteriorate the dispersion [7,9,11]. The change of the structure of the molybdena phase, which accompanies the lower dispersion, has been monitored with several techniques, such as, Raman [2,7,9], IR [2], and XPS [7,11].

Both spreading of crystalline $MoO_3$ (*macrospreading*) and spreading of dispersed molybdena phases (*microspreading*) have been studied by several authors. In this work we present a study on the (*micro*)spreading behavior of novel $MoO_3$-on-$SiO_2$ catalysts prepared by deposition-precipitation of $Mo^{3+}$ from homogeneous solution. The preparation of these samples has been described elsewhere [18]. The trivalent precursor induces an enhancement of the interaction between the aqueous molybdenum precursor and the support. As a result, no crystallites are formed at a $MoO_3$ loading of 5.6 wt%. Data obtained with several characterization techniques, such as, Raman and EXAFS exhibit the high dispersion of the silica-supported molybdena. In spite of the overwhelming number of publications pointing to the reluctance of spreading of molybdena, it will be shown that the molybdenum oxide phase in $MoO_3/SiO_2$ catalysts tends to spread over the $SiO_2$ surface under certain circumstances. The role of water turns out to be crucial in this spreading phenomenon.

## 2. Experimental

### PREPARATION

The $MoO_3$-on-$SiO_2$ sample was prepared by deposition-precipitation of $Mo^{3+}$ from a homogeneous solution onto $SiO_2$ (Aerosil 200 V, Degussa) and has been described elsewhere [18]. It has previously been shown that the use of this alternative precursor leads to highly dispersed catalysts. After filtering off, washing, and drying at 393 K in air, the sample was calcined in air at 723 K for 72 hours.

### CHARACTERIZATION

The loading of the sample was 5.6 wt% $MoO_3$ (determined with Inductively Coupled Plasm (ICP)). X-ray diffraction patterns did not disclose any crystallinity. No particles could be discerned in Transmission Electron Microscopy (TEM). Though $Mo^{3+}$ was used as a precursor, only $Mo^{6+}$ was present in the calcined sample, as evidenced by XPS measurements.

X-ray Absorption Spectroscopy (XAS), and *in situ* laser Raman spectroscopy were used to investigate the behavior of the $MoO_3/SiO_2$ catalysts under hydrated (ambient) and dehydrated conditions.

The Raman apparatus consists of a Triplemate spectrometer (Spex, Model 1877) coupled to an optical multichannel analyzer (Princeton Applied Research, Model 1463) equipped with an intensified photodiode array detector (1024 pixels, cooled to 238 K). For the Raman study under ambient conditions, the sample was pressed onto KBr and spun at 2000 rpm. The *in situ* Raman spectrum was recorded from a stationary sample pressed into a self-supporting wafer (no KBr). A modified version of an *in situ* cell, developed by Wang et al. [19], was used. Ultra-high purity, hydrocarbon-free oxygen (Linde Gas) was purged through the cell. In a typical experiment, the sample was heated to 773 K in 20 minutes and held at 773 K for 30 minutes. The sample was cooled down to 333 K in 45 minutes. At this temperature the *in situ* Raman spectrum was recorded. The acquisition time used per scan was 30 seconds and 25 scans were averaged. To minimize fluorescence, the sample was recalcined for 2 hours at 773 K in dry air prior to the Raman study. The 514.5 nm line of an argon ion laser (Spectra Physics) was used as excitation source. The laser power at the sample was 15–40 mW.

The X-ray absorption spectra (Extended X-ray Absorption Fine Structure (EXAFS) and X-ray Absorption Near Edge Structure (XANES)) were recorded at EXAFS station 9.2 of the S.R.S. at Daresbury, U.K. The station was operated with a double crystal monochromator, Si(220), detuned to 50% intensity to minimize the presence of higher harmonics in the beam. The measurements were carried out in the transmission mode with optimized ion chambers to measure the radiation intensity. Data were collected at each energy for 1s, and results from 6 scans were averaged to minimize high- and low-frequency noise. The samples were pressed into self-supporting wafers (each with an absorbance of approximately 2.5) and mounted in an *in situ* EXAFS cell [20]. The spectra were recorded under helium atmosphere at 77 K. To investigate the influence of dehydration, spectra of both the fresh sample after calcination (Mo6F) and after thermal pretreatment (Mo6P) were recorded. The thermal pretreatment consisted of heating (5 K/min) the sample to 673 K under a 20% $O_2$/He flow, followed by a 2 hours isothermal treatment at 673 K and cooling down under the same atmosphere.

Standard procedures were used to extract the EXAFS data from the measured absorption spectra. Normalization was done by dividing the absorption intensities by the height of the absorption edge and subtracting the background by using cubic spline routines [21]. The final EXAFS function was obtained by averaging the individual background-subtracted and normalized EXAFS data. The data analysis was performed on an isolated part of the data obtained by an inverse Fourier transformation over a selected range in R-space [21]. Experimental references were used for the data analysis: $Na_2MoO_4$ for the Mo-O, and $MoS_2$ for the Mo-Mo interaction. Details of these references are described elsewhere [22].

## 3. Results

The Raman spectra of the 5.6% $MoO_3/SiO_2$ (code: Mo6) sample under ambient condition (Mo6F) and after *in situ* dehydration (Mo6P) are shown in fig. 1. The silica support possesses Raman features at ~820 and 457 $cm^{-1}$ (siloxane linkages), 605 and 488 $cm^{-1}$ (three and four fold siloxane rings) and 1050 $cm^{-1}$ (asymmetric mode of the Si-O-Si linkages). The Raman bands at ~820, ~600, and ~480 $cm^{-1}$ region are thus assigned to $SiO_2$. The complete absence of sharp bands at 997, 819, 663, 335 and 281 $cm^{-1}$, which are characteristic of crystalline $MoO_3$, reveals that both under ambient condition and after *in situ* dehydration, the supported molybdenum oxide is present as a dispersed silica-supported phase. Under ambient conditions, the Raman spectrum exhibits bands at 944, 880, and 220 $cm^{-1}$, which best match those of hydrated, octahedrally coordinated $Mo_7O_{24}^{6-}$ clusters [23]. The observed Raman bands are accordingly assigned as follows: 944 $cm^{-1}$ (Mo=O symmetric stretching mode), 880 $cm^{-1}$ (asymmetric Mo-O-Mo stretching mode), 380 $cm^{-1}$ (Mo=O bending

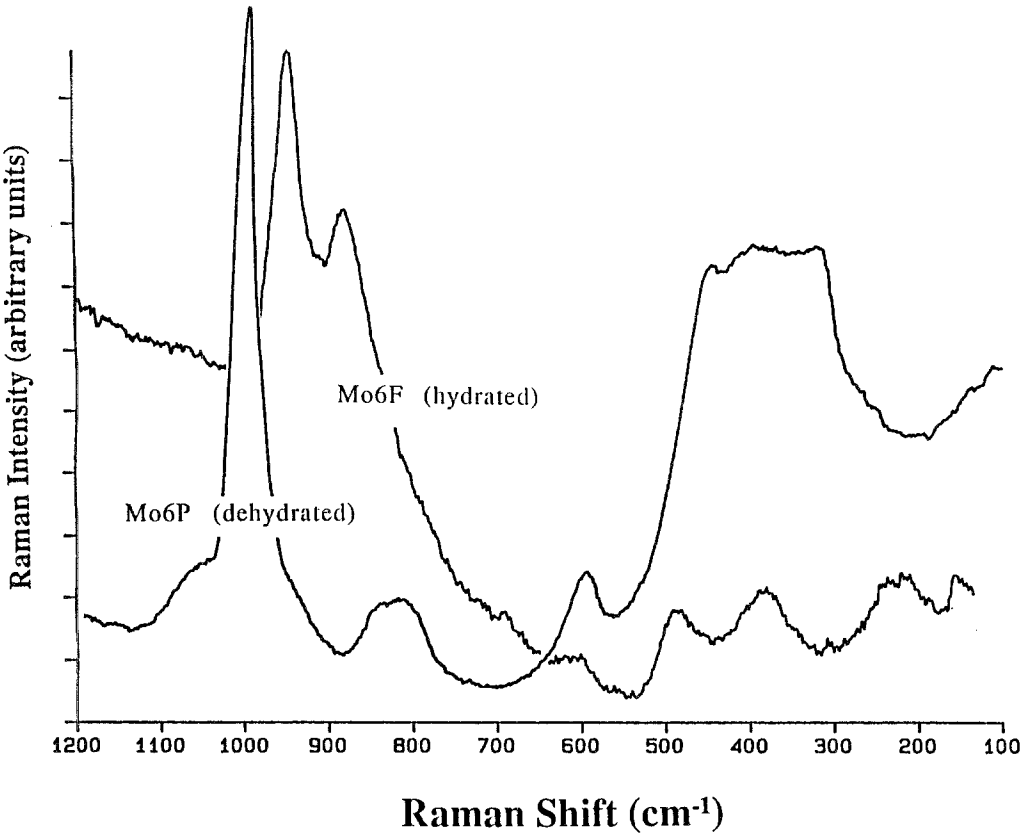


Fig. 1. Raman spectra of Mo6 under ambient conditions (Mo6F) and after thermal pretreatment (Mo6P).

mode) and 220 $cm^{-1}$ (Mo-O-Mo bending mode). Especially the band at 220 $cm^{-1}$ (Mo-O-Mo bending) is diagnostic for the presence of hydrated polymolybdate species under ambient conditions [24].

Dehydration causes a drastic change of the supported molybdenum oxide structure as indicated by the Raman spectrum recorded under dehydrated conditions. The Mo=O stretching mode shifts from 944 to 986 $cm^{-1}$ and the Mo=O bending mode moves from $\sim 380$ to $\sim 310$ $cm^{-1}$. The asymmetric Mo-O-Mo stretching mode at 880 $cm^{-1}$ and the Mo-O-Mo bending mode at 220 $cm^{-1}$ disappear. A similar single sharp band has recently been observed in the *in situ* Raman spectra of $MoO_3/Al_2O_3$, $MoO_3/ZrO_2$ and $MoO_3/TiO_2$ [25] after dehydration. The presence of only one sharp band indicates that the surface molybdenum oxide species is mono-oxo (one short Mo=O bond). A di-oxo species with two equivalent Mo=O bonds would exhibit at least two bands in the stretching region (symmetric and antisymmetric stretching mode), while two nonequivalent Mo=O bonds would display at least two Mo=O symmetric stretching modes and additional antisymmetric stretching modes [26]. In addition to the changes in the molybdenum oxide Raman bands upon dehydration, also the Raman features of silica become visible at $\sim 1050$, $\sim 815$, 605 and 350–500 $cm^{-1}$. The fact that these silica bands are more pronounced under dehydrated conditions indicates that the Raman cross section of the dehydrated molybdenum surface species is much smaller than the cross section of the hydrated molybdenum oxide cluster. Thus, under dehydrated conditions the Raman features of the silica support are no longer overshadowed by the bands of the molybdenum oxide species.

The *in situ* Raman spectrum does not give a clear indication whether this mono-oxo species is octahedrally or tetrahedrally coordinated. However, octahedrally coordinated mono-oxo molybdate species are quite common (e.g. $MoO_3$), whereas no tetrahedrally coordinated mono-oxo molybdate species are known [26]. It is therefore likely that the mono-oxo surface species has a (distorted) octahedral coordination of the $Mo^{6+}$ cation. This dehydrated species is isolated since no bands in the Mo-O-Mo bending region ($< 250$ $cm^{-1}$) are observed.

Progress has recently been made in determining the molecular structures of supported metal oxide species by applying the diatomic approximation method, presented by Hardcastle et al. [27]. They proposed an empirical stretching frequency/bond length correlation by considering each metal-oxygen bond as a totally independent oscillator.

The frequency of the terminal Mo=O bond is related to the interatomic distance by eq. (1) [27].

$$\nu_{Mo=O} = 32895 \exp(-2.073 R_{Mo=O}). \quad (1)$$

Based upon this diatomic approximation method, a mono-oxo molybdate species with the following structure can be envisioned in Mo6P: a distorted octahedrally coordinated molybdenum with one short Mo=O bond, four Mo–O

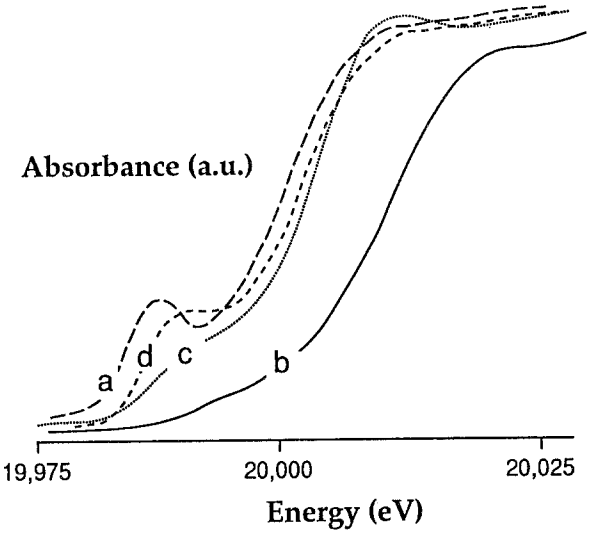


Fig. 2. XANES spectra of: a) $Na_2MoO_4$, b) $MoO_3$, c) Mo6F and d) Mo6P.

bonds in the octahedral base and one long, opposing Mo–O bond. The latter Mo–O bonds would be linked to the $SiO_2$ structure. Using eq. (1), the 986 $cm^{-1}$ stretching mode complies with a Mo=O bond distance of 1.692 ($\pm$0.016) Å, while 944 $cm^{-1}$ corresponds to $R$(Mo=O) = 1.713 ($\pm$0.016) Å.

EXAFS and XANES spectra of the 5.6 wt% $MoO_3/SiO_2$ catalyst were recorded before and after thermal pretreatment (20% $O_2$/He flow (100 ml/min) at 673 K during 2 hours). The XANES-spectra of two reference compounds, $Na_2MoO_4$ (a) and $MoO_3$ (b) and the fresh (Mo6F) (c) and the thermally pretreated (Mo6P) (d) catalyst are shown in fig. 2. The pre-edge peak around 20,000 eV is attributed to the formally forbidden transition 1s $\rightarrow$ 4d. The transition probability of this electronic excitation depends on the local symmetry of the molybdenum atom. In $MoO_3$ ($O_h$) the transition is only slightly allowed, due to the distortion of the octahedral coordination. The lack of a center of inversion in the coordination sphere of the perfectly tetrahedrally surrounded molybdenum atoms in $Na_2MoO_4$ ($T_d$) is the cause of the higher transition probability and, thus, the presence of the pre-edge peak. The pre-edge peak of Mo6F is almost absent, similar to $MoO_3$. It is assumed that the molybdenum atoms in the fresh sample have a (distorted) octahedral coordination. A more distinct pre-edge peak arises in Mo6P. It does, however, not correspond to the higher peak in $Na_2MoO_4$. Apparently, the coordination of the molybdenum atoms in the catalyst changes upon thermal treatment.

Analysis of the EXAFS spectra supports the assumption of a change of the structure of the molybdena species during drying. The $k^1$ weighed $\chi(k)$ of Mo6F and Mo6P is represented in fig. 3. The differences between Mo6F and Mo6P are demonstrated by the $k^2$ weighed Fourier transformation (fig. 4). Both the magnitude (envelope function) and the imiginary part (oscillating function

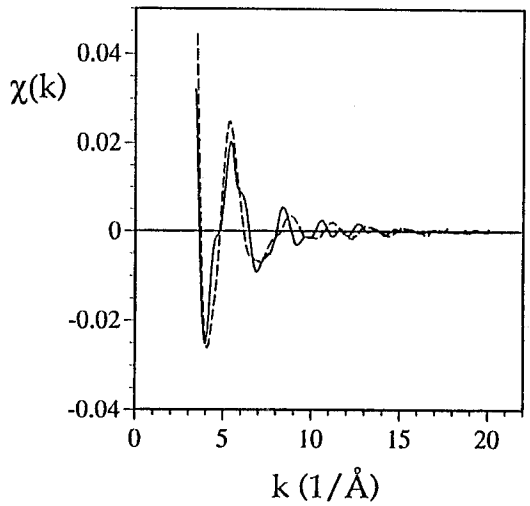


Fig. 3. Raw EXAFS data ($k^1$ weighed) of Mo6F (solid line) and Mo6P (dotted line).

within the envelope) show significant dissimilarities. A $k^2$ weighed Fourier transformation was chosen to emphasize the differences in the more distant shells. Both the Mo-Mo contributions at $3.0 < R$ (Å) $< 4.0$ and the Mo-O shells ($1.6 < R$ (Å) $< 2.3$) change enormously after dehydration.

Some preliminary results of the EXAFS data analysis will be presented here. Analysis of the first shell (Mo-O) of Mo6P was carried out with an isolated part of the EXAFS data. The range for the forward Fourier transformation was $3.69 < k$ (Å$^{-1}$) $< 14.89$, while the inverse transformation interval was $0.26 < R$

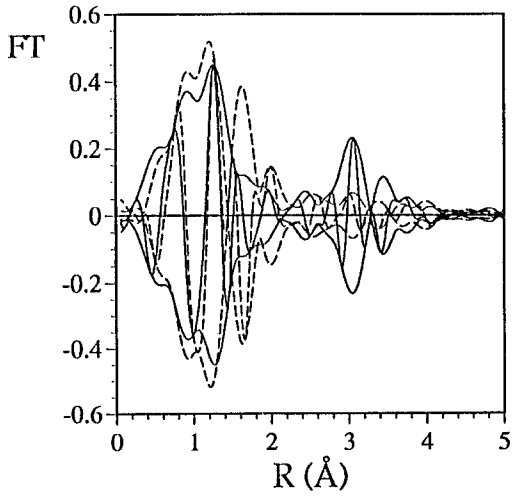


Fig. 4. Magnitude (envelope) and imiginary part (oscillations within envelope) of the Fourier transformation ($k^2$ weighed, $3.63 < k$ (Å$^{-1}$) $< 14.89$) of the raw EXAFS data of Mo6F (solid line) and Mo6P (dotted line).

Table 1
Parameters of the fit ($k^1$ weighed, $4.00 < k$ (Å$^{-1}$) $< 13.5$ and $0 < R$ (Å) $< 4.0$) on the Mo-O coordination of Mo6P

| Shell | $N$ Coordination number | $\Delta\sigma^2$ (Å$^2$) Debye-Waller factor | $R$ (Å) Distance | $E^0$ (eV) Inner potential correction |
|---|---|---|---|---|
| Mo-O | 1.27 | −0.00353 | 1.690 (±0.02) | −17.07 |
| Mo-O | 4.92 | 0.00425 | 1.843 (±0.02) | −5.14 |
| Mo-O | 1.49 | 0.00267 | 1.993 (±0.02) | 9.48 |

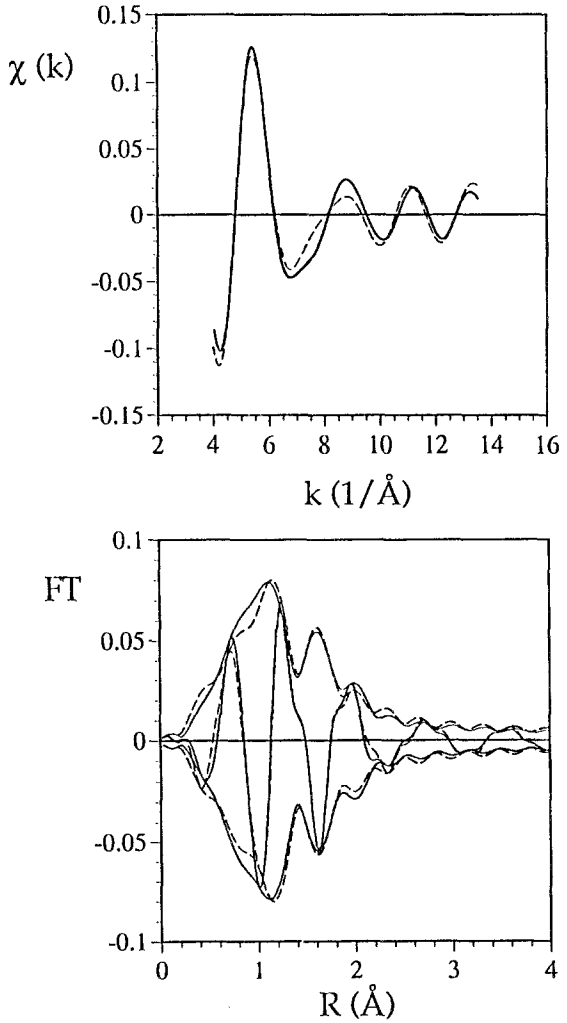


Fig. 5a. Isolated EXAFS ($k^1$ weighed, $0.26 < R$ (Å) $< 2.30$) of Mo6P (solid line) and fit (dotted line). b. Magnitude (envelope) and imiginary part (oscillations within envelope) of the Fourier transformation of the isolated EXAFS ($k^1$ weighed, $4.0 < k$ (Å$^{-1}$) $< 13.5$) of Mo6P (solid line) and fit (dotted line).

Table 2
Parameters of the fit ($k^1$ weighed, $4.00 < k$ (Å$^{-1}$) $< 14.0$ and $2.0 < R$ (Å) $< 5.0$) on the Mo-Mo coordination of Mo6F

| Shell | $N$ Coordination number | $\Delta\sigma^2$ (Å$^2$) Debye-Waller factor | $R$ (Å) Distance | $E^0$ (eV) Inner potential correction |
|---|---|---|---|---|
| Mo-Mo | 0.87 | −0.00008 | 3.368 (±0.02) | 2.48 |
| M0-Mo | 0.76 | 0.00096 | 3.469 (±0.02) | 0.87 |
| Mo-Mo | 1.64 | 0.00506 | 3.606 (±0.02) | −1.72 |
| Mo-O | 5.79 | 0.02668 | 2.459 (±0.02) | −1.20 |

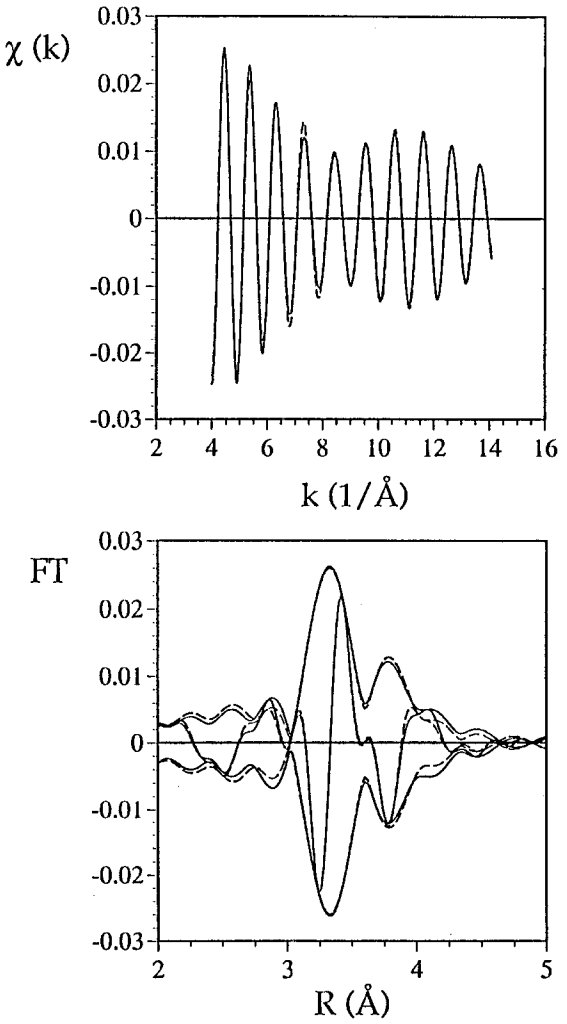


Fig. 6a. Isolated EXAFS ($k^{-1}$ weighed, $2.62 < R$ (Å) $< 4.79$) of Mo6F (solid line) and fit (dotted line). b. Magnitude (envelope) and imiginary part (oscillations within envelope) of the Fourier transformation of the isolated EXAFS ($k^1$ weighed, $4.0 < k$ (Å$^{-1}$) $< 14.0$) of Mo6F (solid line) and fit (dotted line).

(Å) < 2.30. The coordination parameters for the fit, obtained with three Mo-O contributions, are listed in table 1. The number of allowed free parameters ($N_f$) equals 13.3., whereas 'he number of free parameters (12) is lower than $N_f$.

The results of this fit are presented in fig. 5a ($k$-space) and 5b ($R$-space). Approximately one oxygen neighbor at short distance (the terminal Mo=O) is found in this analysis. This coordination number and the corresponding Mo-O distance are consistent with the Raman results that predict a $R_{Mo=O}$ of 1.692. The negative Debye-Waller factor for the first Mo-O shell, indicating a lower disorder than the reference, can be explained by the higher bond strength of Mo=O compared to Mo-O in $Na_2MoO_4$. The analogous fit on Mo6F (not shown) resulted in a slightly higher value for $R_{Mo=O}$: 1.708.

Analysis of the shells in the $3.0 < R$ (Å) $< 4.0$ interval enabled us to investigate the size of the molybdenum oxide cluster before and after dehydration. The Mo-Mo coordination in this $R$-region determines the 'framework' of the cluster. This part of the EXAFS of Mo6F was separated by a forward Fourier transformation over $3.59 < k$ (Å$^{-1}$) $< 14.50$ and a reverse transformation in the $2.62 < R$ (Å) $< 4.79$ interval. $N_f$ for this analysis is, thus, 16.1. The results of the fit are shown in table 2.

The fits are presented in fig. 6a ($k$-space) and 6b ($R$-space). The shape of the envelope of $\chi(k)$ in fig. 6a witnesses the *high-z* character of the scatterer, i.e. Mo-Mo. The total Mo-Mo coordination number ($\sum N_{Mo\text{-}Mo}$) amounts 3.27, distributed over 3 distances. The high value for the $\Delta\sigma^2$ of the Mo-O in this analysis is due to contribution of more Mo-O shells, heavily disordered in this cluster. The $N_f$, however, does not allow a more profound analysis of these scatterers. The corresponding analysis of the Mo-Mo contribution in Mo6P yields dramatically different results. The value found for $\sum N_{Mo\text{-}Mo}$ in Mo6P amounts only 0.2. The sharp decrease of $\sum N_{Mo\text{-}Mo}$ after dehydration of the sample points to a collapse of the molybdenum oxide cluster.

## 4. Discussion

It is clear from the Raman and XAS results that a modification of the structure is induced by thermal dehydration of a 5.6 wt% $MoO_3/SiO_2$ catalyst. Unequivocal evidence for the spreading or 'break up' of the polymolybdate clusters is provided by the strong reduction of $\sum N_{Mo\text{-}Mo}$ and the shift of the terminal Mo=O band in Raman from 944 to 986 cm$^{-1}$ after thermal pretreatment. The sharp decrease of $\sum N_{Mo\text{-}Mo}$ indicates a collapse of the 'framework' of the molybdenum oxide cluster as present in the hydrated state. This implies that the molybdenum atom have dispersed. The shift of the $\nu_{Mo=O}$ in Raman seems to point at the same feature: the molybdenyl sites in the polymolybdate cluster (944 cm$^{-1}$) change into isolated mono-oxo sites (986 cm$^{-1}$). The Mo-O-Mo chains, characteristic for the polymolybdate structure, must have been

broken up to provide the isolated molybdenum sites. This is indeed evident in the Raman spectrum from the disappearance of the bands at 880 and 220 $cm^{-1}$, indicative of the stretching and bending modes of the Mo-O-Mo vibration respectively. The disappearance of the band at 880 $cm^{-1}$ is very clear; the decrease of the Mo-O-Mo bending mode at 220 $cm^{-1}$, however, is less clear due to the high background. The Mo=O bond lengths as derived from EXAFS correspond well to the values found by application of Hardcastle's relationship [27]. A shortening of the terminal Mo=O bond is found upon dehydration: $R_{Mo=O}$ decreases from 1.708 to 1.690 as found by EXAFS analysis, whilst the Raman spectra predicted values of 1.713 and 1.692 respectively. The high bond strength in Mo=O is reflected by the negative value for $\Delta\sigma^2$ in the analysis.

Thermal treatment appears to alter the coordination of molybdenum atoms. The transition from the polymolybdate structure to the isolated molybdenum sites coincides with a change of the molybdenum-oxygen coordination sphere. The chemical coordination of molybdenum is a slightly distorted octahedron, due to the Jahn-Teller effect in the polymolybdate cluster (Mo6F). The peak in the XANES-region at 19,984 eV ($1s \rightarrow 4d$) increases upon thermal treatment. As derived from the intensity of the pre-edge peak, the local coordination of molybdenum in Mo6P must be in between the slightly distorted octahedron ($O_h$), as in $MoO_3$-bulk and Mo6F, and the perfect tetrahedron ($T_d$), as in $Na_2MoO_4$. A heavily distorted octahedral coordination is the most probable option, since no tetrahedrally coordinated mono-oxo molybdenyl species (as derived from the Raman band at 986 $cm^{-1}$) are known in literature.

The break-up of the polymolybdate structure is presumably caused by the removal of water from the sample. An oligomeric cluster, such as $Mo_7O_{24}^{6-}$, is stabilized in aqueous solution by protons or other cations. The equivalent cluster on the surface of $SiO_2$ is stabilized by protons as well, i.e., the cluster contains surface hydroxyl groups under ambient conditions. Upon thermal treatment, however, water is removed from the cluster by condensation of vicinal hydroxyl groups. The destabilized cluster breaks down due to lack of coordinating oxygen atoms. A structural change (spreading of the cluster over the surface of $SiO_2$) can accomplish the replenishment of the coordination sphere. The presence of some Si-OH groups on the $SiO_2$ surface benefits spreading.

The spreading of the molybdenum oxide phase reported in this work does not proceed when $MoO_3$ is badly dispersed or not in contact with the support, because the removal of water from a molybdena crystallite irreversibly leads to the formation of $MoO_3$. This can be explained in terms of competition between the formation enthalpy of the $MoO_3$-lattice and the gain of entropy, obtained by spreading. Leyrer et al. [9] explain the spreading phenomena of $MoO_3$ on $Al_2O_3$ with the surface free energy contributions ($\gamma\ \Delta A$) of the bulk phase and the spreaded phase. Obviously, this model is not applicable to this study since no

bulk $MoO_3$ is present and no data are available for the surface free energy of the clusters.

The so called 'bad' interaction between silica and molybdenum oxide, leading to coalescence thus only applies for badly dispersed $MoO_3$-$SiO_2$ samples.

## References


[1] N. Kakuta, K. Tohji and Y. Udagawa, J. Phys. Chem. 92 (1988) 2583.
[2] S.R. Stampfl, Y. Chen, J.A. Dumesic, C. Niu and C.G. Hill, J. Catal. 105 (1987) 445.
[3] G.A. Tsigdinos, H.Y. Chen and B.J. Streusand, Ind. Eng. Chem. Prod. Res. Dev. 20 (1981) 619.
[4] Y. Barbaux, A.R. Elamrani, E. Payen, L. Gengembre, J.P. Bonnelle and B. Grzybowska, Appl. Catal. 44 (1988) 117.
[5] M. Anpo, M. Kondo, Y. Kubokawa, C. Louis and M. Che, J. Chem. Soc., Faraday Trans. 1, 84(8) (1988) 2771.
[6] S.R. Seyedmonir, S. Abdo and R.F. Howe, J. Phys. Chem. 86 (1982) 1233.
[7] J.M. Stencel, J.R. Diehl, J.R. d'Este, L.E. Makovsky, L. Rodrigo, K. Marcinkowska, A. Adnot, P.C. Roberge and S. Kaliaguine, J. Phys. Chem. 90 (1986) 4739.
[8] J. Leyrer, M.I. Zaki and H. Knözinger, J. Phys. Chem. 90 (1986) 4775.
[9] J. Leyrer, D. Mey and H. Knözinger, J. Catal. 124 (1990) 349.
[10] T. Machej, J. Haber, A. Turek and I.E. Wachs, to be published.
[11] L. Rodrigo, A. Adnot, P.C. Roberge and S. Kaliaguine, J. Catal. 105 (1987) 175.
[12] H. Jeziorowski and H. Knözinger, J. Phys. Chem. 83(9) (1979) 1166.
[13] J.A.R. van Veen and P.A.J.M. Hendriks, Polyhedron 5 (1986) 75.
[14] C.T.J. Mensch, J.A.R. van Veen, B. van Wingerden and M.P. van Dijk, J. Phys. Chem. 92 (1988) 4961.
[15] Y. Okamoto and T. Imanaka, J. Phys. Chem. 92 (1988) 7102.
[16] H. Praliaud, J. Less Common Metals 54 (1977) 387.
[17] P. Sarrazin, B. Mouchel and S. Kasztelan, J. Phys. Chem. 93 (1989) 904.
[18] E.T.C. Vogt, A.J. van Dillen, J.W. Geus, J.J.P. Biermann and F.J.J.G. Janssen, in: *Proc. 9th I.C.C.*, eds. M.J. Phillips and M. Ternan, Vol. 4, Calgary, 1988, p. 1976.
[19] L. Wang and W.K. Hall, J. Catal. 82 (1983) 177.
[20] F.W.H. Kampers, T.M.J. Maas, J. van Grondelle, P. Brinkgreve and D.C. Koningsberger, Rev. Sci. Instr. 60 (1989) 2635.
[21] J.B.A.D. Van Zon, D.C. Koningsberger, H.F.J. Van 't Blik and D.E. Sayers, J. Chem. Phys. 82 (1985) 5742.
[22] S.M.A. Bouwens, R. Prins, V.H.J. de Beer and D.C. Koningsberger, J. Phys. Chem. 94 (1990) 3711.
[23] W.P. Griffith and P.J.B. Lesniak, J. Chem. Soc. (A) (1969) 1066.
[24] G. Deo and I.E. Wachs, J. Phys. Chem. accepted.
[25] T. Machej, J. Haber, A.M. Turek and I.E. Wachs, Appl. Catal. 70 (1991) 115.
[26] N. Nakamoto, *Infrared and Raman spectroscopy of Inorganic and Coordination Compounds* (Wiley, New York, 1978).
[27] F.D. Hardcastle and I.E. Wachs, J. Raman Spectrosc. 21 (1990) 683.